Experimental Characterization of a Lightweight Unmanned Aerial Radiation Detection System equipped with a "Flat Panel" gamma detector.

Tancioni P., Berger P., Chandra R., Gendotti U.

Abstract

The capability of performing radiological monitoring of large areas using a lightweight, rapidly mountable gamma detection system is demonstrated. The system was designed to deliver radiological information such as count rate, dose rate and gamma energy spectra to first responders in response to a nuclear / radiological incident. The "Flat Panel" gamma detector, developed by Arktis Radiation Detectors, relies on plastic scintillation and Silicon Photomultiplier light readout: this solution maximizes performance in terms of efficiency per unit weight, while being highly insensitive to electromagnetic fields, vibrations, and mechanical shocks. With a single flight autonomy of more than 20 minutes, the capability of scanning large areas in radionuclide-localization missions is demonstrated by means of field tests performed at the Spiez CBRN Laboratory in Switzerland. In each test, gamma-emitting radionuclide sources with activities from hundreds of MBq to few GBq and energies ranging from 60 keV to 1.3 MeV have been deployed in a field of 15'000 m^2 and flight patterns at different speed and altitude are carried out in order to assess detection limits. Dose rate heat-maps are generated for different incident gamma energies to validate a dose rate calculation algorithm based on spectroscopic analysis. The measurement results show that the system can reliably localise radionuclide sources in large-area scans in less than 20 minutes, while providing dosimetric and spectroscopic information to first responders to allow real-time assessment of radiological risks.

1. Introduction

Using Unmanned Aerial Vehicles (UAVs) for surveillance and environmental monitoring creates new possibilities for first responders in emergency scenarios, enabling remote assessment and intervention operations such as visual inspections, search and rescue, exclusion zone definition, and many other applications. By avoiding operators to manually perform these actions, the use of UAVs equipped with different payloads has seen a significant increase in the last decade [1-2]. The use of unmanned platforms for radioactive material detection and identification brings many advantages: compared to human-operated manual procedures, it markedly minimises health risks for first responders in case of accidents involving radiological contamination, radioactive source search operations, or nuclear accidents. Traditional radiation monitoring techniques are based on hand-held detection systems, that can result in a significant radiation exposure for the first responders.

Additionally, UAVs can monitor large areas in a timeframe that is generally orders of magnitude lower than what required by manually operated devices, especially in difficult-to-access environments where the operation of ground vehicles is precluded. Moreover, thanks to the reproducibility of flight missions, UAV radiation detection system can bring numerous advantages in routine and periodic environmental radiation survey missions.

However, in order to operate UAVs on large areas avoiding contact with ground obstacles (trees, buildings), the minimum altitude above ground level (AGL) is generally limited. The intensity of a radiation field generated at ground level by a surface contamination or a point-like radionuclide source decreases with the square of the distance. Therefore, high-sensitivity detectors are needed to achieve an optimal trade-off between detection limits and velocity of the UAV. However, devices able to detect and identify gamma-emitting radioactive materials are usually characterized by high density, resulting in heavy detection systems. Since the weight of the detection system is limited by the maximum allowed payload of the UAV, the solution entails maximizing detection sensitivity per unit weight.

Numerous studies have been carried out with the goal of discussing and characterising the application of UAVs equipped with radiation detectors, highlighting the many advantages arising from the deployment of these instruments in environmental survey, contamination assessment, source localisation scenarios [3-6]. Among these works, it is generally acknowledged how the sensitivity of the detector plays a key role in the capability of the system to perform high speed, large area survey missions while giving the operators fundamental information to assess the radiological risk in real time.

In this work, a lightweight, highly portable, high-sensitivity UAV radiation detection system is presented and characterized through source-localisation experimental tests. The detection unit consists of thin plastic scintillator tiles, with the scintillation light read-out by an array of Silicon Photomultipliers (SiPMs) distributed over the active volume as to maximize the light collection. Using plastic scintillator as a detection medium, the sensitivity to gamma radiation per unit weight is maximized. Additionally, this material can be manufactured in arbitrary shapes and volumes, allowing the design of a payload-specific detection unit depending on the type of UAV in use for different applications. Moreover, additional benefits arise from the use of SiPMs for light read-out: they are robust, lightweight, insensitive to vibrations and electromagnetic fields. For this reason, this technology is better suited for UAV applications with respect to traditional light-readout devices such as Photomultiplier Tubes (PMTs), which are heavier, particularly sensitive to mechanical shocks and electromagnetic fields and require high voltage. In Section 2, materials and instrumentation are described in detail. In Section 3, the source-localisation scenarios and experimental tests performed at Spiez CBRN Laboratory in Switzerland are described.

In conclusion, Section 4 presents the test results, showing how the presented UAV detection system can detect and localize radionuclide sources over large areas in a timeframe of minutes, while giving the operator information about the source's energy signatures and dose rate field.

2. Materials and Methods

2.1 Gamma detection system

The "Flat Panel Gamma" (FPG) detection system is designed and manufactured by Arktis Radiation Detectors [7]. It consists of thin and compact tiles of plastic scintillator surrounded by an array of solid-state light readout chips (Silicon Photomultipliers). Detailed information about geometry of the tiles and position of the SiPMs array are proprietary and will not be discussed in this work. The geometry of the tiles and the position of the light-sensitive devices is designed to maximize scintillation light collection, enabling the system to maximize sensitivity and to preserve information about energy signatures of the incoming gamma radiation. For each gamma event depositing energy into the scintillator volume, the scintillation light signal is detected by the SiPMs and filtered with a coincidence logic for noise reduction. If the coincidence requirement is fulfilled, the electronic signal generated by the SiPMs is processed and digitized by the on-board electronics. The Time-over-Threshold (ToT) of this signal is measured (i.e., the time the signal is above an adjustable threshold) and distributed over a histogram of digital channels that are proportional to the energy deposited by the gamma ray interaction in the scintillator.

In a previous work, an energy calibration of the ToT histogram has been performed and used to demonstrate the spectroscopic capabilities of the detector, as well as a dose rate calibration showing accuracy of approximately 90% for an energy range of 60 keV – 1.3 MeV [8]. Customs configurations of the scintillator tiles are available from the manufacturer. In this study, scintillator dimensions of (250 x 150 x 14) mm were used, for a total payload weight of 1.8 kg.

The detector case is also equipped with a LIDAR distance sensor for altitude above ground level (AGL) monitoring, and a camera for image acquisition. The FPG detection system is showed in Figure 1.

Figure 1. The Flat Panel Gamma detector by Arktis Radiation Detectors comprises flat scintillator panels read out by solid state "Silicon Photomultiplier" electronics.

2.2   UAV

A commercial quadcopter drone model Astro manufactured by Freefly Systems was used in this study [9]. The system is highly portable: it can be moved in a single box which can also house the FPG detection system already assembled and ready to measure. The choice of this system was mainly motivated by its compactness and attainability of fast-response flight missions: the time required from opening the box to the UAV's take off was measured to be less than two minutes, with the entire procedure being doable by a single operator. Two Lithium-ion batteries with 175 Wh capacity deliver power to the motors and to the USB output that provides power and connection. The autonomy of the system with the FPG detection system installed (i.e., maximum payload) was tested to be 20-23 minutes. In Figure 2, a picture of the UAV equipped with the FPG detection system is shown.

Figure 2. Astro drone equipped with the FPG detection system offers high sensitivity for a system its size.

The UAV system is equipped with a flight control software developed by Auterion, which also provides a mission control software, both running on an on-board Linux mission computer. This software enables the user to define flight missions and pre-set parameters like altitude, speed, and trajectory of the drone. Completely autonomous missions can be created by the operator, while a "return to land" function is selectable in case an immediate stop of the mission is necessary. The UAV can also be operated in full manual mode through the dedicated ground station. The real-time correction for the UAV's height and position is achieved by an on-board multi-band GNSS module.

The FPG detector is connected to the UAV via USB connector that provides power and exchanges data with the mission computer. Communication with the ground station is also carried out by the on-board mission computer which enables real-time data processing. The computer forwards data as MAVLink messages via the same long-range radio link used to control the UAV. The ground control station forwards the MAVLink messages via User Datagram Protocol (UDP) to be received by one or multiple computers displaying the data. In Figure 3, the communication infrastructure diagram is shown.
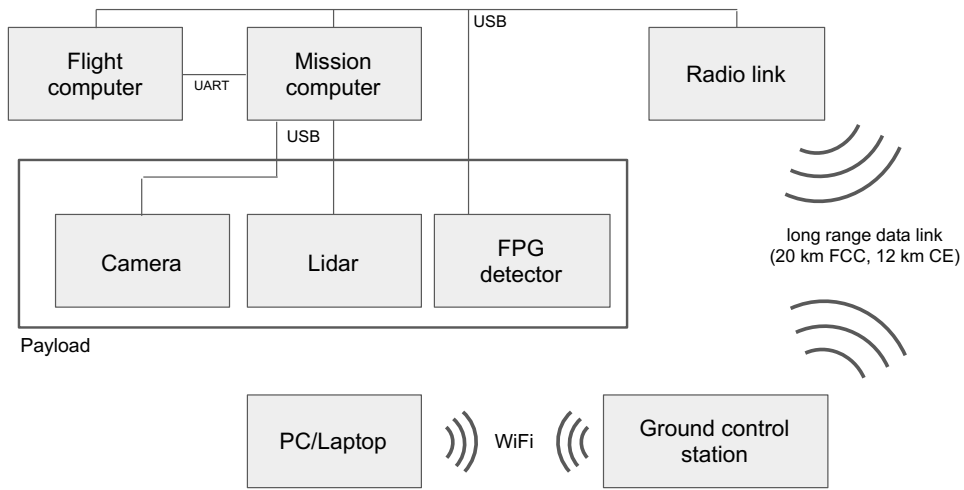
Figure 3. Schematic of the UAV system and connection to the FPG detection system.

3 Flight tests

3.1   Survey area and radionuclide sources

The flight tests were performed in the military training field of CBRN Laboratory of Spiez (Bern, Switzerland). The training field has an area of approximately 15'000 m^2.
Sealed radionuclide sources were positioned on the ground to simulate source search scenarios, with isotopes having emission energy ranging from 60 to 662 keV. A list of the isotopes used in the tests is shown in Table 1, with their activities and main emission energies.

Source ID	Isotope	Main emission line [keV]	Activity [MBq]
#1	137-Cs	661.7	3600
#2	137-Cs	661.7	761
#3	241-Am	59.5	1820
#4	133-Ba	356.0	458

Table 1. List of radionuclide source activities used in tests.

3.2   Set-up of the flight missions

The radionuclide sources were placed on the ground at different positions and in different combinations. Flight missions were planned through the dedicated software to simulate different scenarios. The concept of operations was defined to provide first a coarse, high speed scan with the goal of gathering data over the entire field in the shortest time, followed by a fine, low speed scan to optimize counting statistics and acquire spectral information about the emission energy of the isotopes. The flight missions were generated as a trajectory mesh covering the target area, with different pre-set values of UAV speed and altitude. An example of the flight pattern outlook is shown in Figure 4. Example of the UAV mission set-up in the dedicated control software.
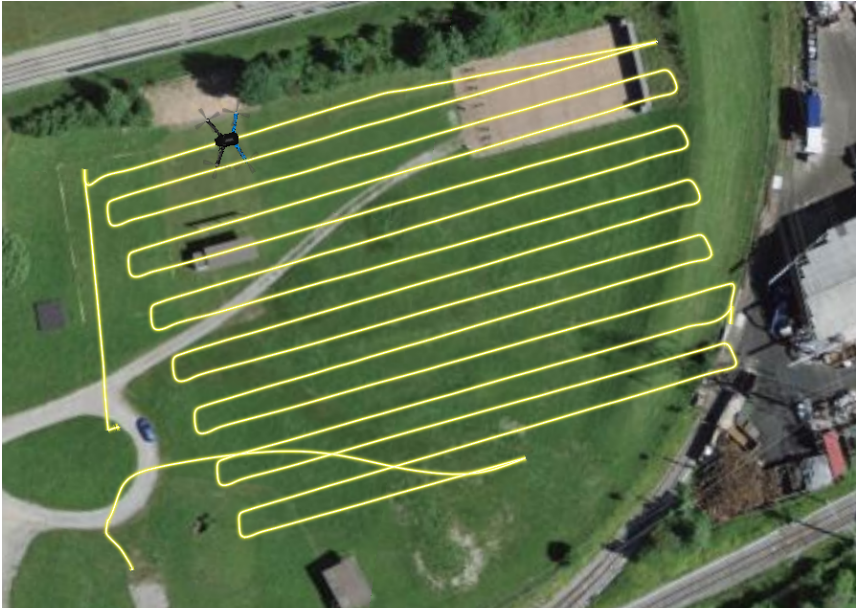
Figure 4. Example of the UAV mission set-up in the dedicated control software.

All the flights were performed in full automated mode. Replacement of the batteries was done in continuous mode (replacing one battery at a time) without the need to switch off the system during the entire duration of the tests and minimizing dead times between flights. A list of the scenarios with respective deployed source, flight altitude, and UAV speed is shown in Table 2. List of source localisation mission scenarios.

Scenario ID	Source ID	Isotope	Altitude above ground [m]	Speed [m/s]
A	background	none	10	4
B	#1	137-Cs	10, 20, 50, 90	4, 6, 10
C	#3	241-Am	10	4
D	#4	133-Ba	10, 20	4, 6
E	#1-#2-#3-#4	all	20, 30, 50, 75	4, 6

Table 2. List of source localisation mission scenarios.

A background acquisition scan was performed prior to the source search missions to assess environmental background count rate and dose rate field of the test area. Afterwards, the radionuclide sources were placed in different positions on the ground and flight altitudes and speeds were adjusted according to the isotope activity and emission energy. In conclusion, all the isotopes were deployed on the field simultaneously and a mixed source scenario was carried out to test the detection system's spatial resolution and its capabilities do discriminate different energy features. The most valuable results obtained from these flight missions are presented in the following section.

10

4 Results

4.1 Scenario A: background mapping

A first background radiation mapping was carried out at a constant speed of 4 m/s and 10 meters AGL. The target area was covered in a total flight duration of 7 minutes and 15 seconds.

Results in term of dose rate are displayed in Figure 5, with an average value of around 0.17 μSv/h and an average count rate of 133 counts per second (cps). A user interface developed by Arktis enables the operator to define the heatmap quantity of interest (count rate or dose rate, average or peak values) and the dimension of the hexagonal area samples according the available counting statistics and to the user's needs.
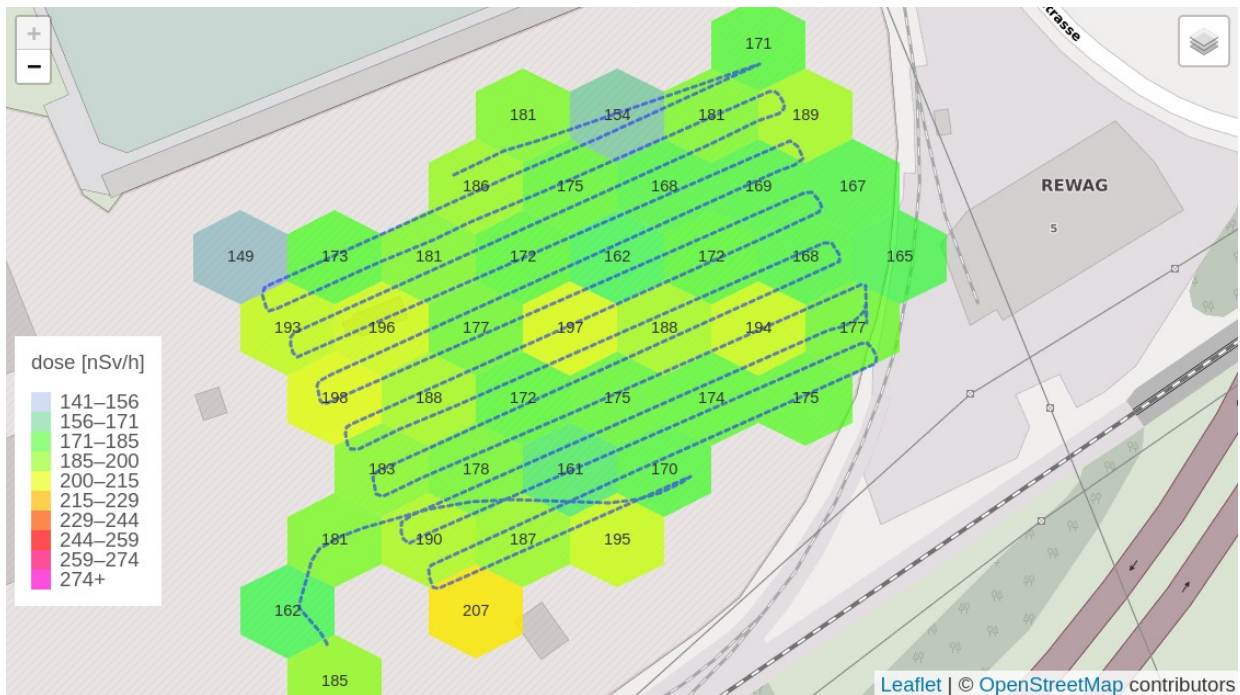
Figure 5. Background radiation dose rate map acquired on the test field (Scenario A).

4.2 Scenario B: Cs-137

For Scenario B, the 3.6 GBq Cs-137 source was positioned in the field and a set of missions with different flights patterns, speed, and altitude values was generated.

The first mission was set-up to achieve a fast, coarse mesh scan over the entire target area, with an altitude of 90 meters and a speed of 10 m/s. With a total flight duration of 4 minutes, a hotspot in the count rate was singled out in the radiation level heatmap

11

with a significance level of approximately 13 standard deviations above background, as shown in Figure 6.

With the goal of acquiring data to optimize spatial resolution, a second fine scan was carried out at a constant speed of 4 m/s and altitude of 10 meters. With a total flight duration of 6 minutes, the source position was determined through data post-processing with an accuracy of around 4 meters. Note that the terms "fast" and "coarse" scan refer to the UAV flight pattern and not to the hexagonal cell size displayed in the user interface, which is an adjustable visualization tool.

Figure 6. Scenario B. Cs-137 source search missions performed with a low-speed, fine scan (left) and with a high-speed, coarse scan (right).

The energy features of the gamma radiation field were investigated by analysing the energy calibrated time-over-threshold histograms acquired by flying over the hotspot at 10 meters altitude. In Figure 7, the spectrum presenting the Cs-137 energy signature is shown. For visualization purposes, reference Compton edge energies are displayed with vertical red lines for the isotopes used in the energy calibration procedure of the FPG detector.
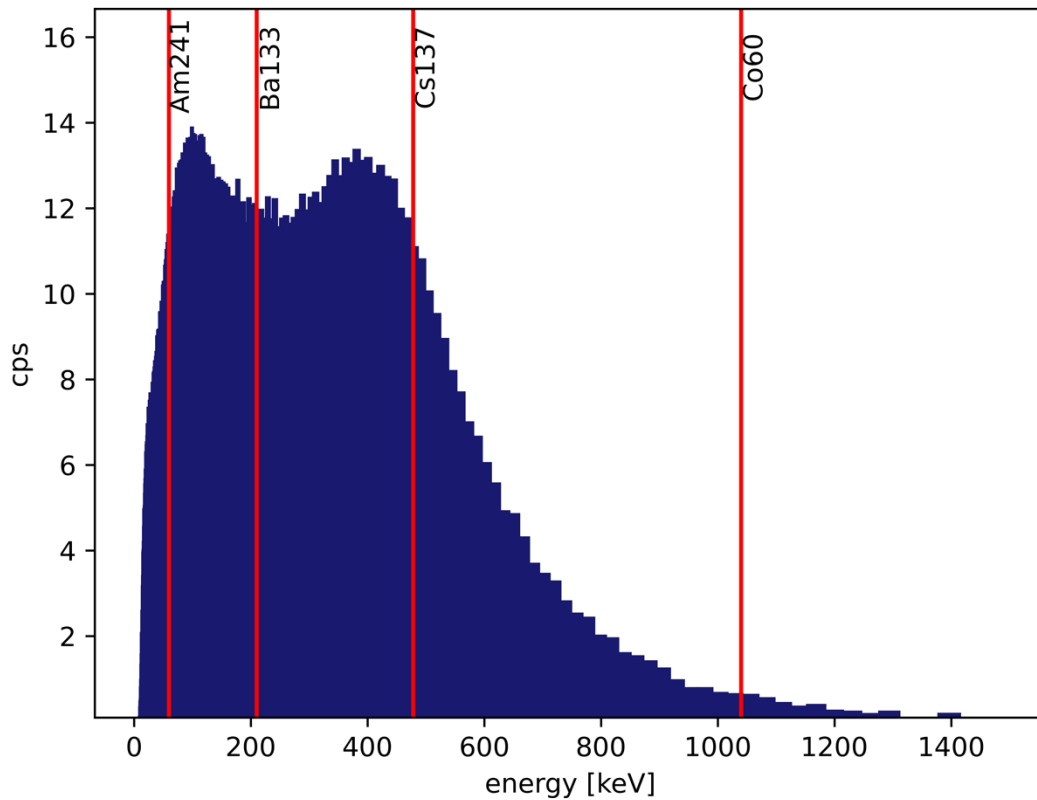
Figure 7. Energy spectrum acquired by flying over the Cs-137 hotspot.

4.3   Scenario C: Am-241

With the goal of testing the system capabilities to localise and characterise isotopes emitting in the low-energy gamma range, the 1.8 GBq Am-241 source was positioned in the field and a mission with constant altitude of 10 meters was set up in order to minimize source-to-detector distance while ensuring safety distance from ground obstacles. To achieve a spatial resolution in the order of a few meters, a UAV speed of 4 m/s was set for this mission.

In Figure 8, the heatmap containing measured count rate levels is shown. After a flight time of 8 minutes the source location was identified with a significance of approximately 8.6 standard deviations above environmental background level.
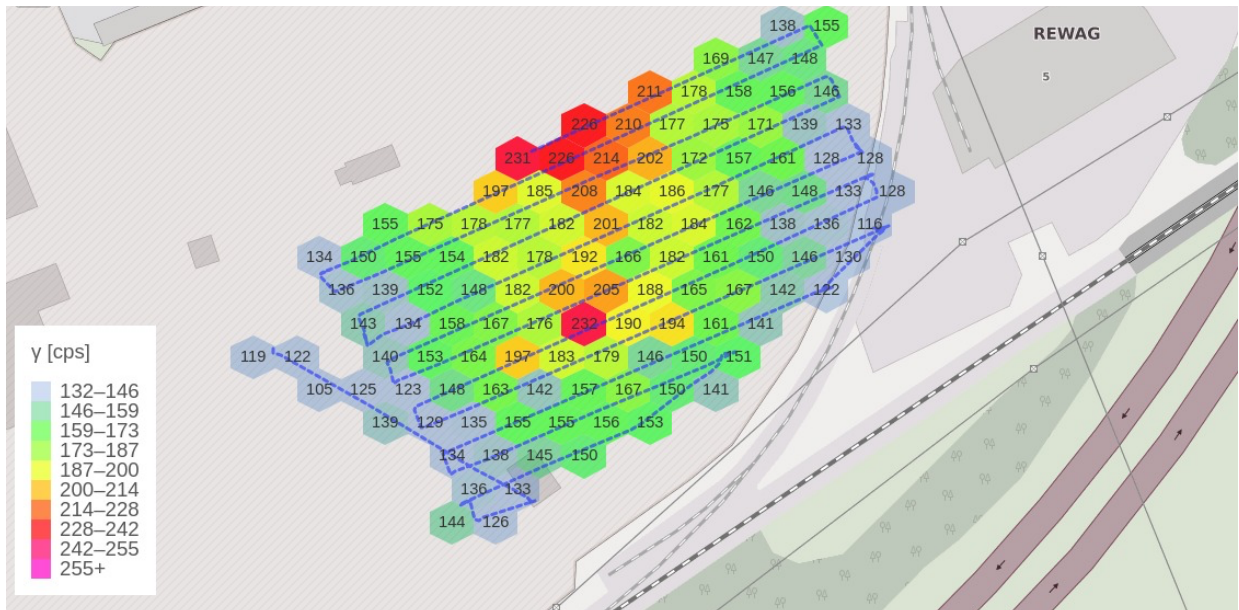
Figure 8. The count rate hot spot generated by the Am-241 source (Scenario C).

The count rate hotspot visible in the central region of the mission pattern corresponds to the position of the Am-241 radionuclide source. In the top part of the grid, the UAV overflew a booth where the rest of the radionuclide sources was stored in a shielded container, showing an additional increase in the count rate before returning to the landing position.

The calibrated time-over-threshold spectra acquired over the hotspot were analysed to investigate the energy features of the incoming gamma radiation. In Figure 9, the spectrum is shown, with a clear signature from the 60 keV gamma ray of Am-241.
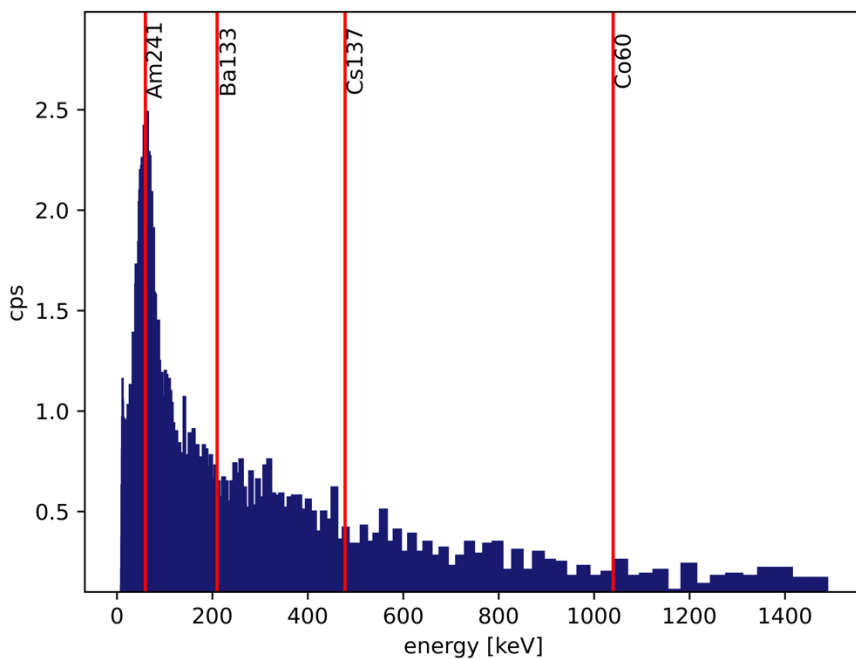

Figure 9. Energy calibrated time-over-threshold spectrum showing Am-241 signature.

4.4   Scenario D: Ba-133

Scenario D was set-up positioning the 458 MBq Ba-133 source on the ground to test the system response to low-mid energy gamma rays (main emission line at 356 keV). Following the same concept of operation of scenario B, two flight missions were set-up: a first coarse scan at 20 meters AGL and 6 m/s speed to obtain a fast overview of the radiation filed over a large area, and a second scan at 10 meters AGL and 4 m/s speed to maximize the measurement's spatial resolution. In Figure 10, the count rate heatmap acquired in the two missions of scenario D is shown.

Figure 10. Count rate heatmap generate in scenario D flight missions. Hotspot shows the position of the Ba-133 radionuclide source.

The first coarse scan could give information about the presence of the hotspot in a flight time of around 3 minutes, while the data analysis of the second, lower speed scan allowed the localisation of the source with an error of less than 5 meters.

4.5   Scenario E: Mixed sources

For the last scenario, all the isotopes used in the previous missions were deployed on the ground at different positions. This mission was set up with the goal of testing the capability of the UAV detection system to discriminate radiation sources with different energies while giving spatial information about their distribution on the field.
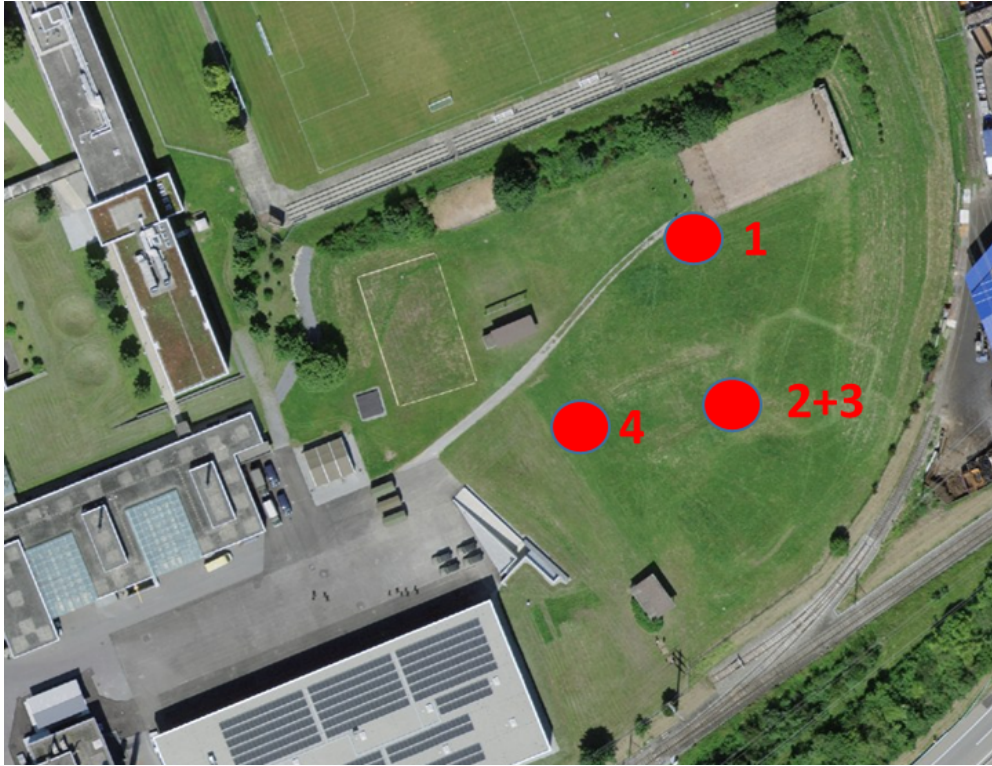The sources position is shown below in Figure 11.

15

Figure 11. Mixed source scenario. Red dots indicate the position of the different radionuclides listed in Table 1. List of radionuclide source activities used in tests.

Scans were carried out at decreasing altitudes from 75 meters to 20 meters. The UAV speed was kept constant at 4 m/s to maximize spatial resolution. Post-process data analysis on the different radiation maps could not allow a clear discrimination between the different sources at altitudes of 75 meters and 50 meters, but two different count rate hotspots were identified by flying at altitudes of 20 and 30 meters, corresponding to hotspots #1 and #2+3 (Figure 12). Flight time for each of the missions was around 12 minutes, and results are shown in Figure 12. Even the lowest altitude scan could not allow any clear spatial discrimination of the hotspot #4: its radiation field was averaged out with the emission resulting from hotspot #2+3 because of their proximity.
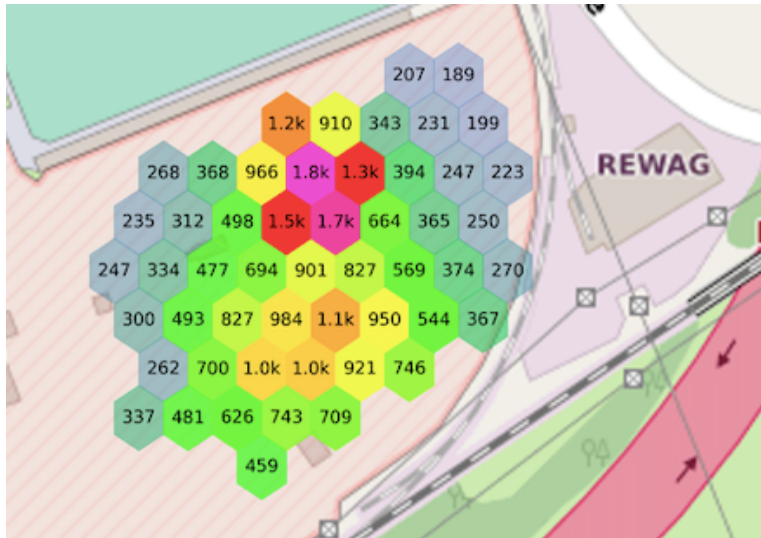
16

Figure 12. Count rate heatmap for Scenario E (all sources present). Two different hotspots are detected in the flight mission with 20 meters AGL and 4 m/s speed.

The spectral information was analysed to check for energy features coming from the different sources. While the Am-241 counting statistics was too low for a clear discrimination of its 60 keV signature in the high Compton continuum resulting from other sources, the Compton edges of Cs-137 and Ba-133 sources are clearly visible (Figure 13).
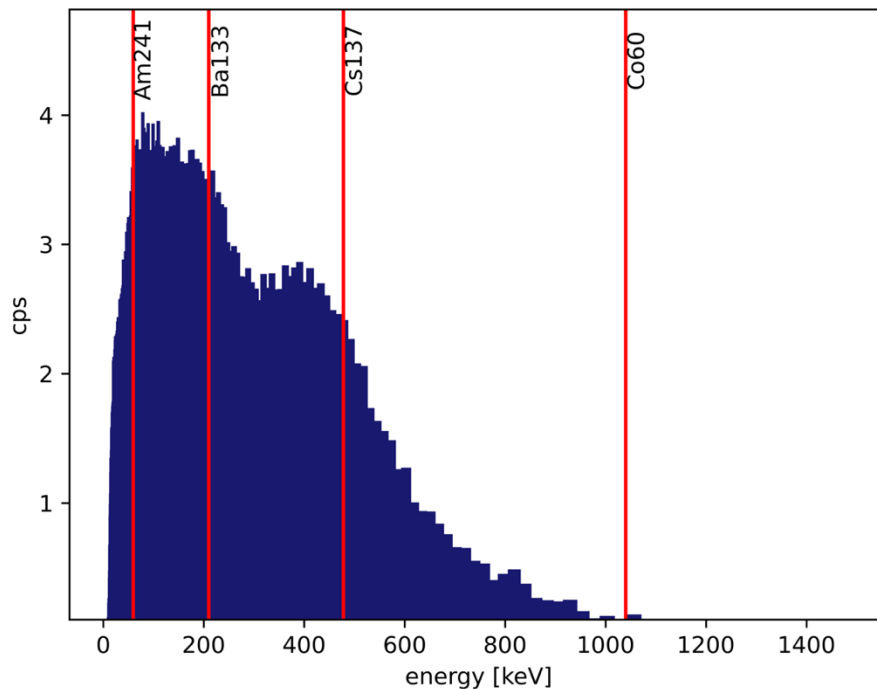

Figure 13. Energy spectrum acquired in the mixed source scenario. Signatures from Cs-137 and Ba-133 are visible.

17

4.6 Dose Rate accuracy

The dose rate capabilities of the detection system were tested by comparison with theoretical dose rate calculated according to the equation (*Knoll, 2010*):

$$\dot{D} = \Gamma \cdot \frac{A}{d^2}$$

where the exposure rate constant Γ depends on the isotopes specific emission energy, usually expressed in (R $\cdot$ cm^2 $\cdot$ mCi^{-1} $\cdot$ h^{-1}), A and d represent isotope activity and the distance from the source, respectively. Values for the constant Γ are from *Smith and Stabin* (2012).

The measured dose rate was compared to the theoretical values for Cs-137 at altitude above ground of 10 and 20 meters. The dose rate map generated in scenario B is shown in Figure 14.
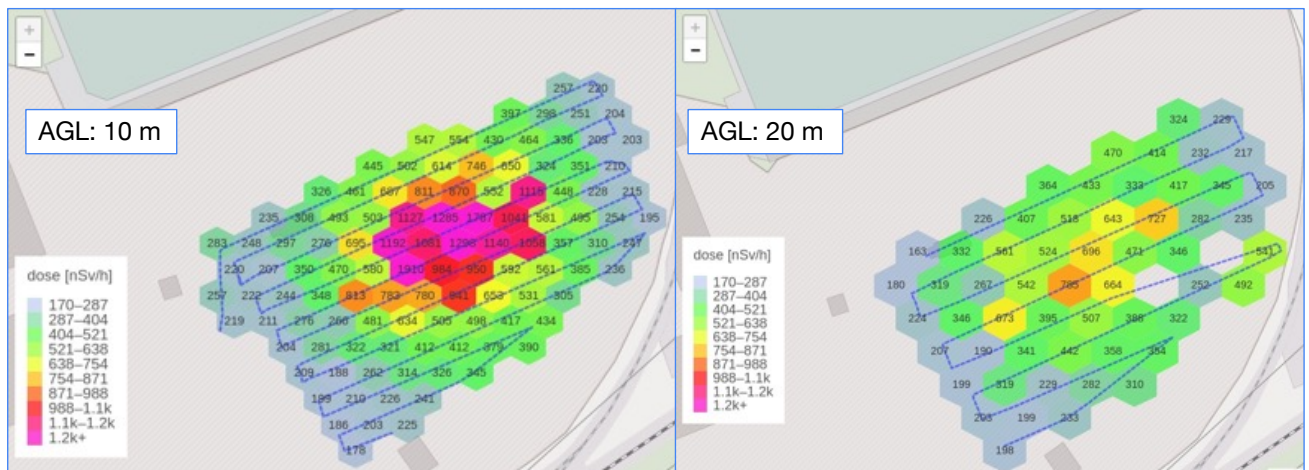

Figure 14. Dose Rate heatmap generated in scenario B, overflying the Cs-137 source.

In Table 3. Dose rate accuracy results., the maximum measured peak dose rate values are reported and the absolute value of error ε with respect to the computed theoretical values is shown.

AGL [m]	Theoretical Dose Rate [µSv/h]	Measured Dose Rate [µSv/h]	Error ε
10	2.64	1.79	47.5%
20	0.81	0.76	6.4%

Table 3. Dose rate accuracy results.

At 20 meters altitude above ground, the absolute difference between the theoretical dose rate and the peak dose rate measured above the source is around 6%. The significant discrepancy between the theoretical and measured dose rates at 10 meters altitude is mainly due to an instability experienced by the automatic altitude correction

system of the UAV: post-processing of the flight data shows that the real average AGL during this flight was around 11.3 meters. By correcting the theoretical value for this difference, the absolute value of this discrepancy decreases to 12.8%.

Additionally, the source was collimated in the upwards direction by a Lead cylinder for radiation protection reasons. The influence of this shielding factor increases with decreasing altitude, where smaller solid angles are subtended by the approaching UAV to the source.

5 Discussion

A lightweight, high-sensitivity gamma detection system using plastic scintillators with a solid-state light readout has been designed and tested for UAV-based radiological source search missions. For such applications, the pre-requisite of a detection system lies in its capabilities to perform fast-response, high counting statistics flights. The restrictions given by the use of a quadcopter UAV set limits to the maximum payload available for the detector. This challenge was tackled by means of optimizing the scintillation light collection to reach the highest sensitivity per unit weight.

The concept of operation of such a system highly depends on the specific goal of the mission. The UAV detection system presented in this work can be transported in a single box by one operator, unpacked and take-off in a timeframe of minutes.

Scenario specific missions can be defined by the user through a dedicated software. A concept of operation for source-search scenarios was tested at a military training field in Spiez CBRN Laboratory (Switzerland). A two-phases procedure was adopted for the definition of flight missions: a first scan at high speed and altitude above ground to give the operator a prompt information about environmental radiation levels, and a second scan at lower speed and altitude to acquire enough spatial information for an accurate localisation of the source in case radiological anomalies were detected in the first scan. Thanks to the optimized light collection of the FPG detection system, spectroscopic data are also available to the operator, providing information about the energy signatures of the gamma radiation field.

The dose rate accuracy of the detection system was tested by comparison with computed theoretical values, showing an accuracy up to 93.6% for Cs-137 at 20 meters altitude.

The capability of localising and characterising radionuclide sources with activities ranging from hundreds of MBq to few GBq, with emission energy from 60 keV to 662 keV, was successfully demonstrated in this study: an area of 15'000 m^2 was scanned within timeframes of minutes, and count rate hotspots generated were singled out with spatial resolution of a few meters. In case of a mixed source scenario, the system was able to perform spatial discrimination between two different hotspots, while providing spectral information of their specific signatures.

References

1. Liew, C.F.; DeLatte, D.; Takeishi, N.; Yairi, T. Recent Developments in Aerial Robotics: A Survey and Prototypes Overview. arXiv 2017, arXiv:1711.10085

2. Radoglou-Grammatikis, P.; Sarigiannidis, P.; Lagkas, T.; Moscholios, I. A Compilation of UAV Applications for Precision Agriculture. Comput. Netw. 2020, 172, 107148

3. Gabrlik P., Lazna T. Simulation of Gamma Radiation Mapping Using an Unmanned Aerial System. IFAC, Volume 51, Issue 6, 2018.

4. Geelen, S.; Camps, J.; Olyslaegers, G.; Ilegems, G.; Schroeyers, W. Radiological Surveillance Using a Fixed-Wing UAV Platform. Remote Sens. 2022, 14, 3908.

5. J.W. MacFarlane et al. Lightweight aerial vehicles for monitoring, assessment and mapping of radiation anomalies, Journal of Environmental Radioactivity, Volume 136, 2014, Pages 127-130, ISSN 0265-931X.

6. D.T. Connor, P.G. Martin, N.T. Smith, L. Payne, C. Hutson, O.D. Payton, Y. Yamashiki, T.B. Scott. Application of airborne photogrammetry for the visualisation and assessment of contamination migration arising from a Fukushima waste storage facility, Environmental Pollution, Volume 234, 2018, Pages 610-619, ISSN 0269-7491.

7. URL: https://www.arktis-detectors.com/fileadmin/downloads/products/Arktis-Flat-Panel-Gamma-Detector-FPG.pdf

8. Tancioni P., Gendotti U. Gamma dose rate monitoring using a Silicon Photomultiplier-based plastic scintillation detector. arXiv 2021, arXiv:2112.03579.

9. URL: https://freeflysystems.com/astro/specs

Acknowledgments